JOURNAL OF MATERIALS SCIENCE 28 (1993) 3594–3600

Structural and physical characterization of the $Li_2O:P_2O_5:CrO_{1.5}$ ion-conducting glasses

W. T. CHIA, B. V. R. CHOWDARI, K. L. TAN
Department of Physics, National University of Singapore, Kent Ridge, Singapore 0511

$Li_2O:P_2O_5:CrO_{1.5}$ glasses containing 40, 50 and 60 mol% Li_2O and a varying P_2O_5-to-$CrO_{1.5}$ ratio have been synthesized. The glass-transition temperature and density increase as P_2O_5 is progressively replaced by $CrO_{1.5}$. The glasses, being green in colour and showing strong optical absorption at 450 nm and 660 nm, contain predominantly Cr^{3+} ions and a relatively small amount of Cr^{6+} ions. The proportions of phosphate species with one, two, and three non-bridging oxygen atoms are determined from Raman spectroscopy results. From X-ray photoelectron spectroscopy (XPS) binding energies of the Li 1s, P 2p, Cr 2p and O 1s core levels are determined. The O 1s spectrum is found to consist of two peaks which are attributed to the P=O, P–O–P, P–O, P–O–Cr, and Cr–O oxygen species. Conductivity of these glasses increases with increasing Li_2O content and with progressive replacement of P_2O_5 by $CrO_{1.5}$. The $0.60Li_2O:0.32P_2O_5:0.08\,CrO_{1.5}$ glass is found to have the highest conductivity, $3.2\times10^{-6}\,\Omega^{-1}\,cm^{-1}$ at 25 °C. Compositional dependence of the conductivity is discussed in relation to variations in the glass structure.

1. Introduction

In recent years solids exhibiting fast ion conduction have been widely studied in view of their potential application as solid electrolytes in electrochemical devices such as batteries, fuel cells, sensors, and electrochemical displays. Glass is one of the important classes of fast ion conductors that are currently being investigated. It has many advantages over its crystalline counterparts, such as isotropic conduction, absence of grain boundaries, ease of fabrication into complex shapes, and wide compositional flexibility allowing optimization of electrolyte properties. In particular, because of the interest in developing high-energy-density lithium batteries, much attention has been devoted to lithium-ion-conducting glasses, including the $Li_2O:P_2O_5$ glasses. It is well known that the mixing of two glass formers often yields glasses with higher conductivity and better thermal stability than the corresponding single-former glasses. It is therefore of academic interest and technological importance to investigate the effect of progressively substituting another glass former for P_2O_5 in the $Li_2O:P_2O_5$ glasses.

The formation of ion-conducting glasses in the $Li_2O:P_2O_5:MoO_3$ and $Li_2O:P_2O_5:WO_3$ systems has already been reported [1–3]. Since Cr, Mo, and W are transition-metal elements belonging to the same column in the periodic table, it is naturally interesting to prepare glasses in the $Li_2O:P_2O_5:CrO_3$ system and compare the structural and physical properties of the various systems. However, it is well known that CrO_3, which is deliquescent, has a low melting point of 198 °C, above which it decomposes into Cr_2O_3 and oxygen by the reaction: $4CrO_3 \rightarrow 2Cr_2O_3 + 3O_2$. In view of the difficulties of handling CrO_3 and the lack of significant differences between glasses prepared from CrO_3 and Cr_2O_3, as observed in our preliminary studies, Cr_2O_3 is used instead of CrO_3 as the starting material. Furthermore, it may be advantageous to use Cr_2O_3 as it has been known to be a conditional glass former.

For the present investigation, the general glass formula adopted is $yLi_2O:(1-y)((1-x)P_2O_5:xCrO_{1.5})$. In this formula, $CrO_{1.5}$ is chosen instead of Cr_2O_3 so that the phosphorous-to-transition-metal ratio may be compared to those in the $Li_2O:P_2O_5:MoO_3$ and $Li_2O:P_2O_5:WO_3$ systems [1–3]. Note that x is equal to $[CrO_{1.5}]/([CrO_{1.5}]+[P_2O_5])$ and gives a measure of the degree of mixing between the two glass formers, P_2O_5 and Cr_2O_3. Glasses with 40, 50, and 60 mol% Li_2O and various values of x are synthesized. Glasses with 70 mol% or higher Li_2O cannot be synthesized because devitrification occurs even when the melts are rapidly quenched. Glasses with less than 40 mol% Li_2O are not synthesized because their conductivities are expected to be very low. The structural and physical properties of the glasses synthesized are determined using various techniques such as differential scanning calorimetry (DSC), ultra violet (u.v.) and visible absorption spectroscopy, Raman spectroscopy, X-ray photoelectron spectroscopy (XPS) and impedance spectroscopy.

2. Experimental procedure

Reagent grade Li_2CO_3, $NH_4H_2PO_4$ and Cr_2O_3 are mixed in the appropriate proportions and melted in a platinum crucible for 15 min. Melting temperature,

0022–2461

which is tabulated in Table I, varies between 1000 °C and 1500 °C depending on composition. Homogeneous melts are obtained on the completion of the following reaction

$$Li_2CO_3 + 2NH_4H_2PO_4 + Cr_2O_3 \rightarrow$$

$$Li_2O + P_2O_5 + Cr_2O_3 + CO_2\uparrow + 2NH_3\uparrow + 3H_2O\uparrow$$

The melts are quenched either between two stainless-steel plates heated to 200 ~ 300 °C (classical quenching) or through a twin roller (rapid quenching). The chemical compositions of the samples are determined by inductively coupled plasma spectroscopy (ICPS).

X-Ray diffraction (XRD) spectra of the samples were obtained on a Philips PW1710 diffractometer using a CrK_α X-ray source ($\lambda = 0.22909$ nm). Thermal analysis was performed on a Shimadzu DSC-50 differential scanning calorimeter at a heating rate of 20 °C min^{-1} under a nitrogen atmosphere.

Absorption spectra were obtained on a JASCO UVIDEC-650 u.v./visible spectrophotometer. Raman spectra were obtained on a JASCO NR-1000 Raman spectrophotometer with an Argon-ion laser using the 90° scattering configuration. XPS spectra were obtained from pulverized samples pressed into discs using a VG Scientific ESCALAB MKII spectrometer with an AlK_α X-ray source ($h\nu = 1486.6$ eV) and with the electron-energy analyser set at a constant pass energy of 20 eV. The binding energies, E_B, were referenced to the C 1s peak ($E_B = 284.6$ eV) resulting from adventitious hydrocarbons present on the sample surfaces.

Ideally, for conductivity measurements, the casted sample should be polished into discs of about 10 mm in diameter and 1 mm in thickness. However, for many compositions the samples broke into small pieces on quenching due to high internal stress. Hence for these compositions the samples were pulverized and pressed into discs of similar dimensions under a load of 5 tonnes. Gold electrodes were then deposited on both sides of the discs and complex-impedance measurements carried out in the frequency range 10 Hz to 500 kHz using a frequency-response analyser (Solartron 1255) and an electrochemical interface (Solartron 1286). Densities of the glasses were determined from the apparent loss of weight in glycerin with an accuracy of $\pm 0.05 \times 10^3$ kg m^{-3}.

3. Results

3.1. Glass formation

The nominal (starting) and actual compositions of the samples are given in Table I. The nominal and actual compositions agree well except for the samples with the nominal compositions $0.60Li_2O{:}0.28P_2O_5{:}0.12CrO_{1.5}$ and $0.50Li_2O{:}0.25P_2O_5{:}0.25CrO_{1.5}$. In these samples, the actual $CrO_{1.5}$ content was found to be lower than expected. This discrepancy is probably due to the presence of undissolved Cr_2O_3 particles found during the chemical analysis. XRD studies show that all samples are amorphous except those of the above two compositions. For these two compositions the classically quenched samples contained crystalline Li_3PO_4 and Cr_2O_3 phases, whereas the rapidly quenched samples contained only a crystalline Cr_2O_3 phase.

Based on the above results, the glass-forming regions in the $0.60Li_2O{:}0.40((1-x)P_2O_5{:}xCrO_{1.5})$, $0.50Li_2O{:}0.50((1-x)P_2O_5{:}xCrO_{1.5})$ and $0.40Li_2O{:}0.60((1-x)P_2O_5{:}xCrO_{1.5})$ series are limited to compositions for which $x \leqslant 0.2$, 0.4, and 0.4, respectively. In the last series, glass could not be synthesized for the

TABLE I Chemical compositions, melting temperatures and glass-transition temperatures, T_g, of the $yLi_2O{:}(1-y)((1-x)P_2O_5{:}xCrO_{1.5})$ glasses

X	Composition (mol %)						Melting temperature (°C)	T_g (°C)
	Nominal			Actual				
	Li_2O	P_2O_5	$CrO_{1.5}$	Li_2O	P_2O_5	$CrO_{1.5}$		
0.0	60.0	40.0	0.0	61.7	38.3	0.0	1000	316
0.1	60.0	36.0	4.0	58.8	37.1	4.2	1200	357
0.2	60.0	32.0	8.0	60.4	32.0	7.6	1200	405
0.3	60.0	28.0	12.0	65.4	30.5	4.1	1300	[a]
0.0	50.0	50.0	0.0	47.3	52.7	0.0	1000	325
0.1	50.0	45.0	5.0	49.5	45.5	5.0	1200	356
0.2	50.0	40.0	10.0	51.0	39.4	9.7	1300	394
0.3	50.0	35.0	15.0	51.1	36.9	12.0	1300	447
0.4	50.0	30.0	20.0	50.5	30.4	19.1	1400	441
0.5	50.0	25.0	25.0	63.0	30.6	6.4	1500	[a]
0.0	40.0	60.0	0.0	40.7	59.3	0.0	1000	283
0.1	40.0	54.0	6.0	41.3	53.1	5.6	1300	354
0.2	40.0	48.0	12.0	40.5	47.4	12.1	1400	397
0.3	40.0	42.0	18.0	40.1	41.9	18.0	1500	454
0.4	40.0	36.0	24.0	40.2	35.3	24.6	1500	550
0.5	40.0	30.0	30.0	–	–	–	1500	[b]

[a] Crystalline/partially-crystalline samples.
[b] Sample not homogeneously melted at 1500 °C.

compositions for which $x > 0.4$ because a homogeneous melt was not obtained. The glasses are transparent and green in colour. The colour of the glasses becomes darker with increasing x. Since the nominal and actual compositions of the glasses agree well, the glasses will be subsequently referred to by their nominal compositions. Measurements were limited to classically quenched samples because the glass-forming limit is not extended by rapid quenching.

3.2. Thermal analysis

Glass-transition temperatures, T_g, of the glassy samples determined from DSC measurements are included in Table I. At constant Li_2O content, T_g increases initially with increasing x. In the 50 mol % Li_2O glasses, T_g reaches a maximum at $x = 0.3$. T_g does not reach any maximum in the 40 and 60 mol % Li_2O glasses, probably because of the limited range of compositions obtained. For glasses with the same x values, however, T_g does not vary appreciably with the Li_2O content. The glass-transition temperatures of the $Li_2O:P_2O_5:CrO_{1.5}$ glasses are high compared to those of the $Li_2O:P_2O_5:MoO_3$ [1] and $Li_2O:P_2O_5:WO_3$ [2] glasses, although the overall T_g behaviour is similar.

3.3. Optical absorption

The u.v. and visible absorption spectra of glasses in the $0.5Li_2O:0.5$ $((1-x)P_2O_5:xCrO_{1.5})$ series are presented in Fig. 1. Absorption bands are observed with maxima around 290 nm, 450 nm and 660 nm, which are respectively attributed to the $^4A_2 \rightarrow {}^4T_1(P)$, $^4A_2 \rightarrow {}^4T_1(F)$ and $^4A_2 \rightarrow {}^4T_2(F)$ transitions of Cr^{3+} ions [4]. The additional structure observed in the $^4A_2 \rightarrow {}^4T_2(F)$ peak could be attributed to the $^4A_2 \rightarrow {}^2T_1$ and $^4A_2 \rightarrow {}^2E$ transitions [4] arising from Fano anti-resonances [5].

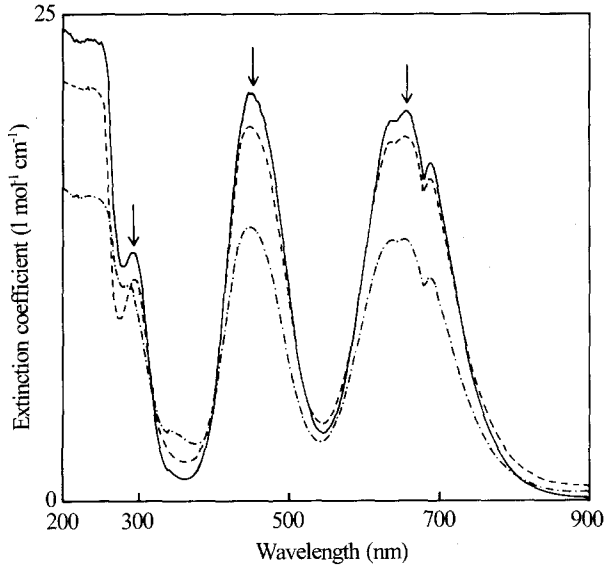

Figure 1 Absorption Spectra of the $0.5Li_2O:0.5$ $((1-x)P_2O_5:xCrO_{1.5})$ glasses: (——) $x = 0.1$, (– – –) $x = 0.2$, and (–·–·–) $x = 0.3$.

As x increases from 0.1 to 0.3, the respective extinction coefficients at the maxima around 450 nm and 660 nm decrease while a small increase in the respective extinction coefficients is observed around 370 nm. The increased extinction coefficient is attributed to Cr^{6+} ions which are known to have strong charge-transfer bands around 256 nm and 370 nm [4]. The above observation suggests that the Cr^{6+}/Cr^{3+} ratio increases with increasing x. However, the fact that the extinction coefficient around 370 nm is small compared to those around 450 nm and 660 nm shows clearly that the Cr ions are present predominantly in the 3+ oxidation state.

3.4. Raman spectroscopy

Raman spectra of glasses in the $0.5Li_2O:0.5((1-x)P_2O_5:xCrO_{1.5})$ series are presented in Fig. 2. The spectra are deconvoluted into Gaussian peaks as previously described [3]. Raman peaks are observed in the regions 550, 705–745, 940–950, 1045–1050, 1120–1172 and 1220–1260 cm^{-1} which are associated with the symmetric stretching vibrations of various structural groupings in the glasses.

The peak at 550 cm^{-1} is associated with Cr^{3+} ions in octahedral co-ordination [6]. This peak is broad and becomes more intense with increasing $CrO_{1.5}$ content. The absence of any Raman peak around 900 cm^{-1}, which is commonly associated with Cr^{6+} ions in tetrahedral co-ordination [6], confirms the conclusion from optical-absorption studies that Cr ions are predominantly in the 3+ oxidation state.

The peak in the 705–745 cm^{-1} region is attributed to the symmetric stretching vibrations of phosphate chains (P–O–P). With increasing x, this peak shifts to higher wavenumbers, a phenomenon which has been attributed to the progressive rupture of P–O–P chains [7]. The peak in the 1220–1260 cm^{-1} region is attributed to asymmetric stretching vibrations of PO_2 groups [8].

The peaks in the 940–950, 1045–1050 and 1120–1172 cm^{-1} regions are attributed to the symmetric stretching vibrations of phosphate tetrahedra with three, two, and one non-bridging oxygen atoms (P–O), respectively [7, 9]. These phosphate tetrahedra are the basic structural units of the Li_3PO_4, $Li_4P_2O_7$, and $LiPO_3$ crystalline phases, and shall be referred to as the Q_3, Q_2, and Q_1 species, respectively. The subscript to Q denotes the number of non-bridging oxygen atoms.

3.5. X-ray photoelectron spectroscopy

Binding energies of the Li 1s, P 2p, Cr 2p and O 1s core-levels are determined from the respective XPS spectra and are tabulated in Table II. The binding energy of Li 1s is almost constant for all the glasses. The binding energy of P 2p shows a slight decrease with increasing Li_2O content and with increasing x. For the Cr 2p spectrum, deconvolution shows that it is well fitted with two peaks with full-width-at-half-maximum (FWHM) of 3.2 and 3.4 eV respectively. This means the Cr ions are present in only one chemical

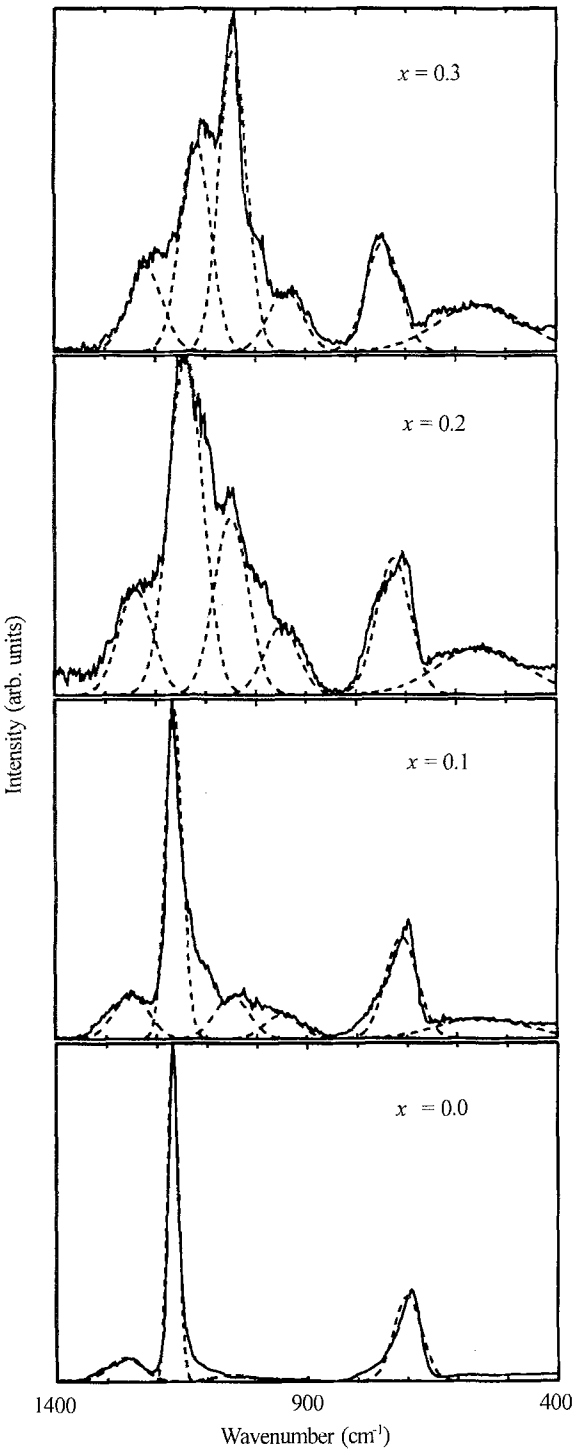

Figure 2 Deconvoluted Raman spectra of the $0.50Li_2O:0.50((1-x)P_2O_5:xCrO_{1.5})$ glasses.

state because the Cr 2p spectrum due to spin-orbit splitting consists of a doublet of $2p_{3/2}$ and $2p_{1/2}$. Since optical-absorption and Raman-spectroscopy results only show evidence of Cr^{3+} ions, the Cr 2p doublet is assigned to Cr ions in the 3+ oxidation state. The Cr $2p_{3/2}$ binding energy remains fairly constant at 578.2 eV, decreasing slightly only in the $0.40Li_2O:0.36P_2O_5:0.24CrO_{1.5}$ and $0.50Li_2O:0.30P_2O_5:0.20CrO_{1.5}$ glasses. This binding-energy value is higher than that found in Cr_2O_3 [10].

On deconvolution, the O 1s spectrum is found to consist of two peaks, both with a FWHM of 2.00 eV. The deconvoluted O 1s spectra of the $0.5Li_2O:0.3P_2O_5:0.2CrO_{1.5}$ glass is shown in Fig. 4 as an example. The lower and higher binding-energy peaks are referred to as the O 1s(1) and 1s(2) peaks, respectively. The fractional peak area of the O 1s(1) peak, $F_{O\,1s(1)}$, also given in Table II, is found to increase with increasing x.

3.6. Electrical measurement

Direct-current conductivities, σ, of the glasses are determined from complex-impedance analysis of the electrical data. Arrhenius plots of $\log\sigma$ against $1000/T$ are found to be linear and well fitted by the Arrhenius equation

$$\sigma = \sigma_0 \exp(-E_a/kT) \quad (1)$$

The logarithm of σ at 25 °C, activation energy, E_a and logarithm of the pre-exponential factor, σ_0 are calculated using linear regression analysis and summarized in Table III. From the data of the $0.50Li_2O:0.45P_2O_5:0.05CrO_{1.5}$ and $0.50Li_2O:0.40P_2O_5:0.10CrO_{1.5}$ glasses, it can be seen that the values of σ obtained from the pulverized-and-pelletized samples are lower than those obtained from the as-casted-and-polished samples by about one order of magnitude. This is due to the lower compactness of the pulverized-and-pelletized samples which is found to be about 80% by weight. Therefore, comparison can only be made between samples of the same physical form. Keeping this in mind it can be seen that σ increases with increasing x and Li_2O content. The increase in σ is accompanied by a decrease in E_a. On the other hand, $\log\sigma_0$ decreases initially as a small amount of P_2O_5 is substituted by $CrO_{1.5}$ but does not seem to vary with further substitution. The $0.60Li_2O:0.32P_2O_5:0.08CrO_{1.5}$ glass is found to have the highest σ of $3.2\times10^{-8}\,\Omega^{-1}\,cm^{-1}$ at 25 °C.

3.7. Density, Li-ion concentration and oxygen-packing density

Densities of glasses in the $0.5Li_2O:0.5((1-x)P_2O_5:xCrO_{1.5})$ series are determined and tabulated in Table IV. It can be seen that density increases with increasing x. Li-ion concentration and oxygen-packing density [11] are calculated from the glass density and nominal composition and tabulated in Table IV.

4. Discussion

4.1. The glass structure

The optical absorption results show that the present glasses predominantly contain Cr^{3+} ions and only a negligible amount of Cr^{6+} ions. Cr ions in conventional glasses are mostly present in the 3+ and 6+ oxidation states. In acidic glasses melted under reducing conditions, the Cr^{6+} content can be substantially suppressed [12, 13]. For the present glasses, it is noted that P_2O_5 is one of the most acidic glass formers and the use of $NH_4H_2PO_4$ as one of the starting materials creates a reducing melting condition. Due to a very large ligand field stabilization energy, Cr^{3+} ions exist only as octahedral complexes in conventional glasses [4]. This is confirmed by the observation of a Raman

TABLE II XPS binding energies of the various core-level electrons and the fractional peak area, $F_{O\ 1s(1)}$, of the $yLi_2O:(1-y)((1-x)P_2O_5:xCrO_{1.5})$ glasses

Composition (mol %)				Binding energies (eV ± 0.1 eV)					
Li_2O	P_2O_5	$CrO_{1.5}$	x	Li 1s	P 2p	Cr $2p_{3/2}$	O 1s(1)	O 1s (2)	$F_{O\ 1s(1)}$
60	40	0	0.0	55.3	133.7	–	531.4	533.0	0.79
60	36	4	0.1	55.3	133.7	578.2	531.3	533.1	0.79
60	32	8	0.2	55.3	133.6	578.0	531.3	533.1	0.87
50	50	0	0.0	55.2	134.2	–	531.4	533.2	0.65
50	45	5	0.1	55.3	134.1	578.1	531.4	533.2	0.69
50	40	10	0.2	55.4	134.0	578.2	531.4	533.2	0.77
50	35	15	0.3	55.4	133.7	578.0	531.4	533.2	0.83
50	30	20	0.4	55.3	133.5	577.5	531.4	533.2	0.86
40	60	0	0.0	55.4	134.5	–	531.7	533.4	0.58
40	54	6	0.1	55.1	134.1	578.2	531.3	533.1	0.62
40	48	12	0.2	55.5	134.1	578.3	531.4	533.2	0.68
40	42	18	0.3	55.5	133.9	578.2	531.4	533.2	0.76
40	36	24	0.4	55.4	133.6	577.8	531.4	533.2	0.83

TABLE III Electrical data of the $yLi_2O:(1-y)((1-x)P_2O_5:xCrO_{1.5})$ glasses

Composition (mol %)					$\log\sigma$ (at 25 °C)	$\log\sigma_0$	E_a (eV)
Li_2O	P_2O_5	$CrO_{1.5}$	x				
60	40	0	0.0	[a]	− 7.15 ± 0.05	3.25 ± 0.11	0.615 ± 0.009
60	36	4	0.1	[b]	− 7.77 ± 0.03	3.00 ± 0.06	0.637 ± 0.005
60	32	8	0.2	[b]	− 7.49 ± 0.07	3.21 ± 0.16	0.633 ± 0.013
50	50	0	0.0	[a]	− 8.49 ± 0.04	3.76 ± 0.12	0.724 ± 0.009
50	45	5	0.1	[a]	− 7.93 ± 0.03	3.15 ± 0.05	0.655 ± 0.004
50	40	10	0.2	[a]	− 7.25 ± 0.03	3.06 ± 0.06	0.610 ± 0.005
50	45	5	0.1	[b]	− 9.11 ± 0.08	2.95 ± 0.17	0.713 ± 0.014
50	40	10	0.2	[b]	− 8.87 ± 0.05	3.24 ± 0.11	0.717 ± 0.009
50	35	15	0.3	[b]	− 8.10 ± 0.03	3.21 ± 0.07	0.669 ± 0.006
50	30	20	0.4	[b]	− 7.83 ± 0.06	3.19 ± 0.14	0.652 ± 0.011
40	60	0	0.0	[a]	− 10.46 ± 0.07	4.08 ± 0.20	0.860 ± 0.016
40	54	6	0.1	[b]	− 10.80 ± 0.24	3.20 ± 0.44	0.828 ± 0.039
40	48	12	0.2	[b]	− 10.21 ± 0.16	3.24 ± 0.30	0.796 ± 0.027
40	42	18	0.3	[b]	− 9.74 ± 0.05	3.02 ± 0.08	0.755 ± 0.007
40	36	24	0.4	[b]	− 9.00 ± 0.03	3.21 ± 0.07	0.723 ± 0.006

[a] As-casted-and-polished sample.
[b] Pulverized-and-pelletized sample.

TABLE IV Density data of the $0.50Li_2O:0.50((1-x)P_2O_5:xCrO_{1.5})$ glasses

Composition (mol %)				Density ($kg\,m^{-3}$)	Li-ion concentration (mole/litre)	Oxygen-packing density (mole/litre)
Li_2O	P_2O_5	$CrO_{1.5}$	x			
50	50	0	0.0	2310	26.9	80.7
50	45	5	0.1	2400	29.1	82.1
50	40	10	0.2	2460	31.0	82.2
50	35	15	0.3	2520	33.1	82.0
50	30	20	0.4	2600	35.7	82.1

band at 550 cm^{-1} which is associated with CrO_6 octahedra. That Cr ions exist mainly in one oxidation state is also supported by the XPS results.

The presence of phosphate tetrahedra with one (Q_1), two (Q_2), and three (Q_3) non-bridging oxygen atoms is revealed by the Raman results. Assuming that all the phosphate tetrahedra have the same scattering efficiency, the concentrations of these species may be taken to be proportional to the areas of the associated Gaussian peaks [3, 7] The compositional dependence of the proportions of the various phosphate species are presented in Fig. 3. It can be seen that at $x = 0.0$, corresponding to the $LiPO_3$ composition, the Q_1 species is the predominant species as expected. As x

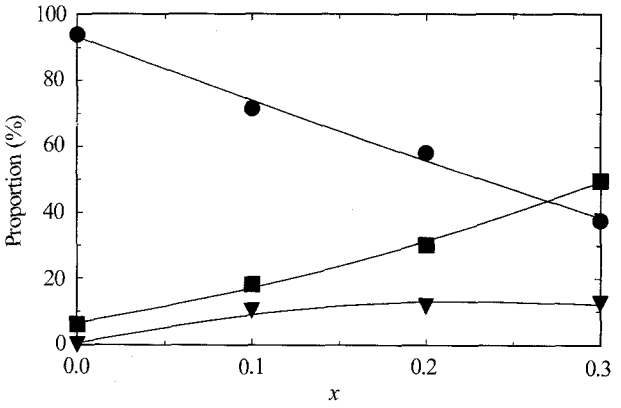

Figure 3 Proportions of the various phosphate species in the $0.50Li_2O:0.50((1-x)P_2O_5:xCrO_{1.5})$ glasses: (●) Q_1 species, (■) Q_2 species, (▼) Q_3 species, and (——) spline-fitting curves.

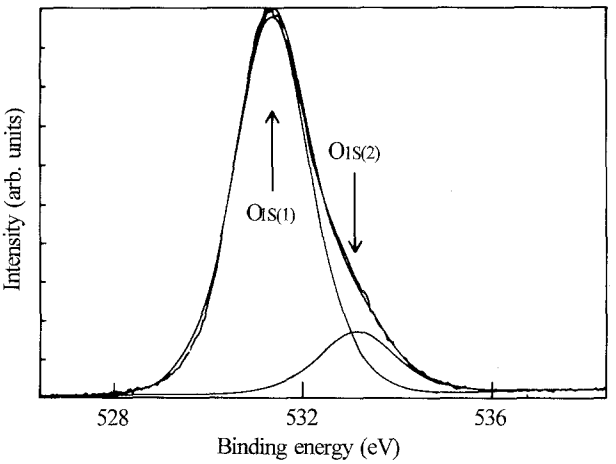

Figure 4 Deconvoluted XPS O 1s spectrum of the $0.5Li_2O:0.3P_2O_5:0.2CrO_{1.5}$ glass.

increases, the proportion of the Q_1 species decreases while the Q_2 and Q_3 species form in increasing proportions. This behaviour closely resembles that in alkali phosphate glasses with increasing alkali-oxide content [7].

A structural model is proposed for the $Li_2O:P_2O_5:CrO_{1.5}$ glasses based on the above observations. It is proposed that these glasses consist of PO_4 tetrahedra and CrO_6 octahedra, sharing corners according to the Zachariasen rules [14]. The CrO_6 octahedra are connected to PO_4 tetrahedra and not to CrO_6 octahedra because of the small x values in these glasses. The CrO_6 octahedra and PO_4 tetrahedra are therefore connected by P–O–P and P–O–Cr linkages. These linkages are modified by Li_2O in the following reactions:

$$Li_2O + P-O-P \rightarrow 2P-O^-Li^+ \quad (2)$$

$$Li_2O + P-O-Cr \rightarrow P-O^-Li^+ + Cr-O^-Li^+ \quad (3)$$

As a result, phosphate tetrahedra with one, two, or three non-bridging oxygen atoms are formed.

According to the above structural model, oxygen species such as P–O–P, P=O, P–O, P–O–Cr, and Cr–O are present in the $Li_2O:P_2O_5:CrO_{1.5}$ glasses. The compositional dependence of the XPS O 1s spectrum may be examined by attributing the O 1s(1) peak at 531.4 eV and the O 1s(2) peak at 533.2 eV in Fig. 4 to these oxygen species. For alkali phosphate glasses, the O 1s binding energies of the P=O and P–O oxygen species were found at around 531.4 eV, while that of the P–O–P oxygen species was found at around 533.2 eV [15]. Hence in the present glasses the P=O and P–O oxygen species contribute to the O 1s(1) peak and the P–O–P oxygen species contributes to the O 1s(2) peak. The O 1s binding energies of the P–O–Cr and Cr–O oxygen species are not known. However, it has been found that the binding energy of a core-level electron increases with increasing effective charge on the emitting atom [16]. Comparing the effective charges on these oxygen species as obtained from their electronegativities, it may be deduced that the P–O–Cr and Cr–O oxygen species have lower binding energies than the P–O–P oxygen species. Thus the O 1s(2) peak may be attributed only to the P–O–P oxygen species. Table II shows that the fractional peak area of the O 1s(1) peak, $F_{O\,1s(1)}$, increases with increasing x for a constant Li_2O content. The fractional peak area of the O 1s(2) peak, given by $1 - F_{O\,1s(1)}$, therefore decreases at the same time implying a decreasing proportion of the P–O–P oxygen species. This is in agreement with the above structural model because more P–O–P linkages are expected to be replaced by P–O–Cr linkages or to be modified by Li_2O as P_2O_5 is progressively replaced by $CrO_{1.5}$.

4.2. The ion conduction

Table IV shows that in the $0.5Li_2O:0.5((1-x)P_2O_5:xCrO_{1.5})$ series, the closeness of packing of the glasses which is measured by the oxygen-packing density remains fairly constant as P_2O_5 is progressively replaced by $CrO_{1.5}$. Therefore, the radius of the "doorway" for ion migration, as envisaged in the Anderson and Stuart model [17], should not vary appreciably. Furthermore, the strain-energy contribution is expected to be small compared to the Coulombic-energy contribution because of the small size of the Li-ion. On the other hand, Li-ion concentration increases as P_2O_5 is progressively replaced by $CrO_{1.5}$ leading to a decrease in the Li-ion separation from 0.395 to 0.360 nm. (Li-ion separation varies as the cube root of the Li-ion concentration.) Since increasing site proximity causes a decrease in the Coulombic-energy barrier [18], the overall activation energy would decrease if variations in the strain-energy barrier are small. This offers a plausible explanation for the increase in conductivity observed in these glasses as P_2O_5 is progressively replaced by $CrO_{1.5}$.

The formation of phosphate tetrahedra with a higher number of non-bridging oxygen atoms, as is evident from the Raman results, offers another possible explanation for the increase in conductivity with increasing $CrO_{1.5}$ content. It is well known that the conductivity of an ion-conducting glass generally increases with increasing concentration of non-bridging oxygen atoms. For instance, the $Li_4P_2O_7$ glass, consisting of the Q_2 phosphate species, is more than a hundred times more conducting than the $LiPO_3$ glass, consisting of the Q_1 phosphate species [18, 19].

Hence the present $Li_2O:P_2O_5:CrO_{1.5}$ glasses are expected to consist of regions of varying conductivities depending on the local non-bridging-oxygen-atom concentrations. Since phosphate tetrahedra with higher numbers of non-bridging oxygen atoms are formed as P_2O_5 is progressively replaced by $CrO_{1.5}$, highly conducting pathways may be formed leading to an increase in the overall conductivity of the glasses.

5. Conclusion

The glass-forming region in the $Li_2O:P_2O_5:CrO_{1.5}$ system is narrow when compared to those in the $Li_2O:P_2O_5:MoO_3$ and $Li_2O:P_2O_5:WO_3$ systems. This is reasonable because Cr_2O_3 has a high tendency to crystallize. However, the Cr_2O_3 content in the present glasses is high compared to those studied before; the Cr_2O_3 content in the $0.40Li_2O:0.36P_2O_5:0.24CrO_{1.5}$ glass is 22 wt %. The incorporation of a large amount of Cr_2O_3 modifies the phosphate glasses both structurally and physically. Based on the results of the optical absorption, Raman and XPS studies, a structural model for the $Li_2O:P_2O_5:CrO_{1.5}$ glasses is proposed, in which the glass network consists of phosphate tetrahedra in various degrees of linkage and Cr^{3+} ions in octahedral coordination. The conductivity of the $Li_2O:P_2O_5:CrO_{1.5}$ glasses increases with increasing Li_2O content and as P_2O_5 is progressively replaced by $CrO_{1.5}$. This is attributed to a decrease in Li-ion separation and the formation of highly conducting phosphate species. The $0.60Li_2O:0.32P_2O_5:0.08CrO_{1.5}$ glass has the highest conductivity: $3.2 \times 10^{-8}\ \Omega^{-1}\,cm^{-1}$ at 25 °C.

References

1. B. V. R. CHOWDARI, K. L. TAN, W. T. CHIA and R. GOPALAKRISHNAN, *J. Non-Cryst. Solids* **128** (1991) 18.
2. B. V. R. CHOWDARI, K. L. TAN, W. T. CHIA and R. GOPALAKRISHNAN, in: "Recent advances in fast ion conducting materials and devices", edited by B. V. R. Chowdari, Q. G. Liu and L. Q. Chen (World Scientific, Singapore, 1990) p. 513.
3. B. V. R. CHOWDARI, K. L. TAN and W. T. CHIA, to be published in *Solid State Ionics.*
4. A. PAUL, "Chemistry of glasses" (Chapman and Hall, London, 1982).
5. A. LEMPICKI, L. ANDREWS, S. NETTLE, B. McCOLLUM and E. I. SOLOMON, *Phys. Rev. Lett.* **44** (1980) 1234.
6. F. D. HARDCASTLE and I. E. WACHS, *J. Mol. Catal.* **46** (1988) 173.
7. M. TATSUMISAGO, Y. KOWADA and T. MINAMI, *Phys. Chem. Glasses* **29** (1988) 63.
8. YA. S. BOBOVICH, *Opt. Spectrosc.* **13** (1962) 274.
9. C. NELSON and D. R. TALLANT, *Phys. Chem. Glasses* **25** (1984) 31.
10. E. DESIMONI, C. MALITESTA, P. G. ZAMBONIN and J. C. RIVIÈRE, *Surf. Interface Anal.* **13** (1988) 173.
11. N. H. RAY, *J. Non-Cryst. Solids* **15** (1974) 423; in: "Ionic polymers", edited by L. Holliday (Applied Science Publishers, London, 1975), p. 369.
12. M. B. VOLF, "Chemical approach to glass" (Elsevier, Amsterdam, 1984).
13. H. SHOLZE, "Glass: nature, structure, and properties" (Springer-Verlag, New York, 1991).
14. W. H. ZACHARIASEN, *J. Am. Chem. Soc.* **54** (1932) 3841.
15. R. GRESCH, W. MÜLLER-WARMUTH and H. DUTZ, *J. Non-Cryst. Solids* **34** (1979) 127.
16. K. SIEGBAHN, C. NORDLING, G. JOHANSSON, J. HEDMAN, P. F. HEDEN, K. HAMRIN, U. GELIUS, T. BERGMARK, L. O. WERME, R. MANNE and Y. BAER, "ESCA applied to free molecules" (North Holland, Amsterdam, 1969).
17. O. L. ANDERSON and D. A. STUART, *J. Am. Ceram. Soc.* **37** (1954) 573.
18. S. W. MARTIN and C. A. ANGELL, *J. Non-Cryst. Solids* **83** (1986) 185.
19. A. PRADEL, T. PAGNIER and M. RIBES, *Solid State Ionics* **17** (1985) 147.

Received 25 May
and accepted 19 November 1992